© 2014. Published by The Company of Biologists Ltd | Development (2014) 141, 1514-1525 doi:10.1242/dev.102426

RESEARCH ARTICLE

A secretory cell type develops alongside multiciliated cells, ionocytes and goblet cells, and provides a protective, anti-infective function in the frog embryonic mucociliary epidermis

Eamon Dubaissi[1], Karine Rousseau[1,2], Robert Lea[1,3], Ximena Soto[1], Siddarth Nardeosingh[1], Axel Schweickert[4], Enrique Amaya[1,3], David J. Thornton[1,2] and Nancy Papalopulu[1,*]

ABSTRACT

The larval epidermis of *Xenopus* is a bilayered epithelium, which is an excellent model system for the study of the development and function of mucosal and mucociliary epithelia. Goblet cells develop in the outer layer while multiciliated cells and ionocytes sequentially intercalate from the inner to the outer layer. Here, we identify and characterise a fourth cell type, the small secretory cell (SSC). We show that the development of these cells is controlled by the transcription factor Foxa1 and that they intercalate into the outer layer of the epidermis relatively late, at the same time as embryonic hatching. Ultrastructural and molecular characterisation shows that these cells have an abundance of large apical secretory vesicles, which contain highly glycosylated material, positive for binding of the lectin, peanut agglutinin, and an antibody to the carbohydrate epitope, HNK-1. By specifically depleting SSCs, we show that these cells are crucial for protecting the embryo against bacterial infection. Mass spectrometry studies show that SSCs secrete a glycoprotein similar to Otogelin, which may form the structural component of a mucus-like protective layer, over the surface of the embryo, and several potential antimicrobial substances. Our study completes the characterisation of all the epidermal cell types in the early tadpole epidermis and reinforces the suitability of this system for the *in vivo* study of complex epithelia, including investigation of innate immune defences.

KEY WORDS: FoxA1, Infection, Mucins, Mucociliary, Otogelin, *Xenopus* epidermis

INTRODUCTION

Epithelia that line internal cavities have several important specialised functions. Such epithelia include the mucosal epithelia of the gut, the mucociliary epithelia of the lung and the secretory epithelia of the kidney. Although their predominant function differs in each case, all of these epithelia have two properties in common: they consist of several different cell types that cooperate to perform the epithelium's primary function, and they are required to act as a protective barrier for internal tissues.

A number of human diseases arise due to damaged or defective mucosal or mucociliary epithelia and they are usually caused by a defect in one of the many cell types that comprise the epithelial tissue. However, this primary defect can have an impact on adjacent cell types, compromising the function of the epithelium as a whole. This is exemplified by cystic fibrosis in the respiratory epithelium and the gut. The cystic fibrosis transmembrane conductance regulator (CFTR), a chloride/bicarbonate transporter, is principally found in serous acinar cells in the submucosal glands of the lungs (Engelhardt et al., 1992). However, mutations in this channel can have indirect effects on neighbouring cells by affecting ionic homeostasis, making mucus thick and sticky and inhibiting clearance by cilia (Houtmeyers et al., 1999). In the gut, CFTR is present in enterocytes but it has been hypothesised that intercellular communication with adjacent goblet cells can affect secretion of mucins through alterations in levels of bicarbonate (Garcia et al., 2009). Thus, understanding how different cell types interact, and the role that each one plays in the integrity of the epithelium, is of paramount importance for understanding the underlying aetiology of epithelial disease.

Epithelial models that are reconstituted *in vitro* tend not to recapitulate the complexity that exists *in vivo*, but experiments in mammalian models are difficult, invasive and expensive. For these reasons, model systems of lower vertebrates, where such epithelia can be readily accessed, have been instrumental in advancing our understanding of mucociliary epithelial development. In recent years, the larval skin of *Xenopus* has been extensively studied because it is known to have a population of motile multiciliated cells (Drysdale and Elinson, 1992). Indeed, research into the ciliated cells in the epidermis of *Xenopus* embryos has yielded a number of important insights that are relevant across different biological systems and disease (Deblandre et al., 1999; Mitchell et al., 2007; Park et al., 2008; Stubbs et al., 2012). For example, the PCP protein, Fritz, has been shown to be crucial in controlling the localisation of the cytoskeletal Septin proteins to the base of cilia (Kim et al., 2010). The same study identified mutations in the human Fritz gene in patients suffering from ciliopathies such as Bardet-Biedl syndrome. This illustrates how findings in a model organism such as *Xenopus* can have direct clinical relevance.

However, if the embryonic *Xenopus* epidermis is to be a truly powerful model of mucociliary and mucosal epithelia, it is necessary to understand and characterise all cell types that comprise it. With this in mind, we, and others, have recently identified the ionocytes. Ionocytes tend to appear in close proximity to the ciliated cells in the larval epidermis and they have a number of pumps and channels

[1]Faculty of Life Sciences, Michael Smith Building, University of Manchester, Oxford Road, Manchester M13 9PT, UK. [2]Wellcome Trust Centre for Cell Matrix Research, University of Manchester, Manchester M13 9PT, UK. [3]The Healing Foundation Centre, University of Manchester, Manchester M13 9PT, UK. [4]University of Hohenheim, Institute of Zoology, Garbenstrasse 30, D-70593 Stuttgart, Germany.

*Author for correspondence (nancy.papalopulu@manchester.ac.uk)

This is an Open Access article distributed under the terms of the Creative Commons Attribution License (http://creativecommons.org/licenses/by/3.0), which permits unrestricted use, distribution and reproduction in any medium provided that the original work is properly attributed.

Received 12 August 2013; Accepted 2 February 2014

Development (2014) doi:10.1242/dev.102426

involved in regulating ionic balance and pH (Dubaissi and Papalopulu, 2011; Quigley et al., 2011). Similar cells are found in human mucosal epithelia, such as the serous cells in the respiratory tract (Loffing et al., 2000) and the enterocytes of the gut (Garcia et al., 2009). Depletion of these cells in the *Xenopus* embryonic epidermis caused a defect in the localisation of basal bodies of neighbouring ciliated cells. This is likely to be due to alteration in pH across the epidermis, which is known to affect the localisation of Dishevelled, a basal body interacting protein (Park et al., 2008; Simons et al., 2009). These findings confirm the power of a multicellular model system in uncovering previously unknown cell-cell interactions that take place *in vivo*.

The *Xenopus* larval epidermis also contains 'goblet cells' that make up the majority of the epithelium and were originally described at an ultrastructural level in electron micrographs (Billett and Gould, 1971). It is generally assumed that they secrete mucins, like their mammalian counterparts; however, no specific mucins have ever been identified in secretions from these vesicles. They are known to secrete a lectin, Xeel, which is proposed to recognise pathogen-associated glycans (Nagata et al., 2003). The glycosaminoglycan, chondroitin sulphate, has also been identified in the goblet cells but its function is not clear (Nishikawa and Sasaki, 1993).

In this study, we identify and characterise an additional cell type in the larval epidermis of *Xenopus tropicalis*. This cell type is small and contains an abundance of large apical secretory vesicles. We adopt the term small secretory cells (SSCs), which has been previously used for cells of similar ultrastructural morphology but unknown function (Hayes et al., 2007). Our data suggest that SSCs are specified by Foxa1, secrete a dense, heavily glycosylated material, are responsible for the innate defence mechanisms of the embryo against pathogen invasion, and complete the characterisation of the embryonic epidermis.

RESULTS

Identification of a new epidermal cell type

The larval *Xenopus* embryonic epidermis has been shown to contain at least three cell types: ciliated cells, ionocytes and goblet cells (Dubaissi and Papalopulu, 2011). To investigate whether there are additional cell types, we combined double fluorescent *in situ* hybridisation using a probe for ciliated cells (*α-1-tubulin*) and a probe for ionocytes (*atp6v1a*), with antibody staining for goblet cells (anti-Xeel) and the nuclear marker, DAPI, at late tailbud stages (stage 32). As Fig. 1A shows, these three cell types do not account for all of the cells in the epidermis and there is at least one more cell type present (examples in yellow circles).

Foxa1 was previously shown to be expressed in a scattered, spotted epidermal distribution by *in situ* hybridisation in *Xenopus laevis* (Hayes et al., 2007) and we confirmed this in *X. tropicalis* (Fig. 1B). Combining *foxa1* with the markers of the other cell types showed that *foxa1* is expressed in the remaining cell type (Fig. 1C,D). With *foxa1* included, no further gaps were present in the staining (Fig. 1D), which led us to conclude that the *foxa1*-positive cells complete the composition of the outer epidermal layer at late tailbud stages. But what are these cells and how do they arise?

The *foxa1*-expressing cell type intercalates into the outer layer at mid-tailbud stages

The epidermal expression of *foxa1* begins after the onset of *foxj1* and *foxi1* expression in ciliated cells and ionocytes, respectively, at about stage 13-14 (supplementary material Fig. S1). Meanwhile, combining markers for ciliated cells, ionocytes and goblet cells at mid-tailbud stages (stage 25) showed that all the outer layer cells are accounted for (data not shown), whereas at late tailbud stages they are not (Fig. 1A). This led us to hypothesise that the *foxa1*-positive cell type intercalates into the outer layer, like ciliated cells

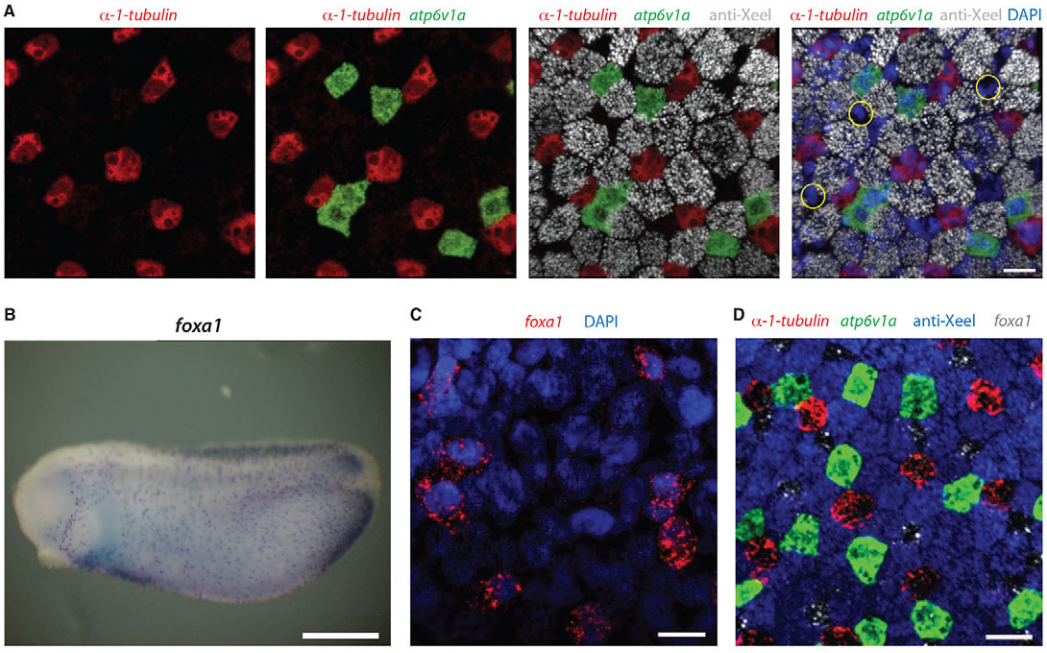

Fig. 1. *foxa1* marks a new epidermal cell type. (A) Double fluorescence *in situ* hybridisation and antibody staining for a ciliated cell marker (*α-1-tubulin*, red), an ionocyte marker (*atp6v1a*, green) and a goblet cell marker (anti-Xeel, grey) on stage 32 embryos. DAPI (blue) is used to mark each cell. At least one cell type (yellow circles) is not stained by these markers. (B) Chromogenic *in situ* hybridisation for *foxa1* on stage 25 embryos shows scattered, spotted epidermal distribution. (C) *foxa1* is epidermally expressed in a subset of DAPI-positive cells. (D) *foxa1* expression (grey) completes the epidermal staining when added to markers of the other cell types at stage 32. Scale bars: 20 μm in A,C,D; 500 μm in B.

Development

Development (2014) doi:10.1242/dev.102426

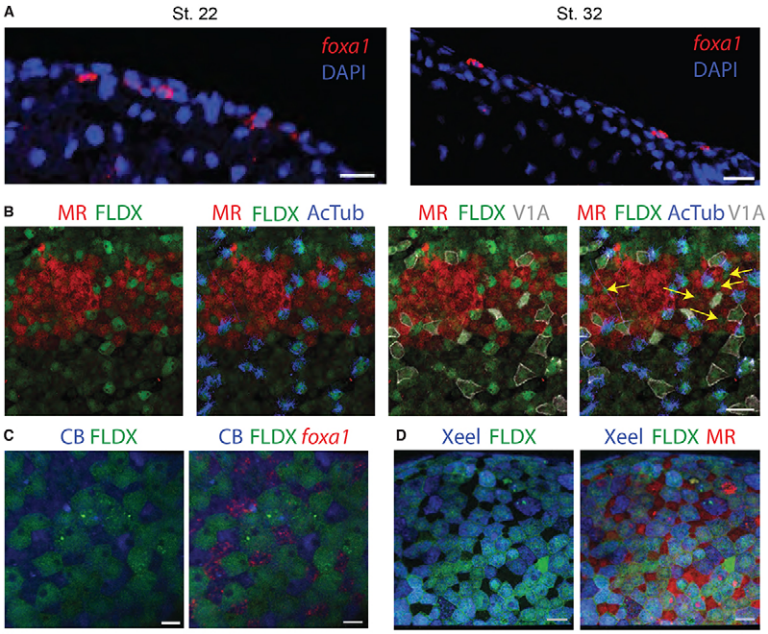

Fig. 2. *foxa1* cells intercalate from inner to outer layer at mid-tailbud stages. (A) Sections of stage 22 and stage 32 embryos stained for DAPI (blue) and *foxa1* (red) by fluorescent *in situ* hybridisation shows that expression changes from inner to outer layer as the embryo develops. (B) Transplant of MR-labelled (red) outer layer epidermal tissue on to FLDX-labelled (green) host embryo and stained using antibodies for ciliated cell marker, acetylated α-tubulin (AcTub, blue) and ionocyte marker, V1a (grey) at stage 32. A cell type (yellow arrows) intercalates from inner to outer layer in addition to ciliated cells and ionocytes. (C) Transplant of FLDX-labelled (green) outer layer epidermal tissue on to CB-labelled (blue) host embryo and stained by fluorescent *in situ* hybridisation for *foxa1* (red) at stage 32. (D) Transplant of FLDX-labelled (green) outer layer epidermal tissue on to MR-labelled (red) host embryo and stained with anti-Xeel antibody (blue). Scale bars: 50 µm in A,B,D; 15 µm in C.

(Deblandre et al., 1999) and ionocytes (Dubaissi and Papalopulu, 2011), but at a later time point.

Indeed, *foxa1* expression changes from inner to outer layer between early and late tailbud stages (Fig. 2A). When performing a transplant of a micro-ruby (MR)-labelled piece of outer layer of one embryo onto a fluorescein-dextran (FLDX)-labelled inner layer of another at gastrula stages (see Materials and methods), there is clearly a cell type (marked by yellow arrows) that intercalates into the outer layer in addition to ciliated cells (anti-AcTub antibody, blue) and ionocytes (anti-V1a, white) by stage 32 (Fig. 2B). To see if *foxa1* cells do indeed intercalate, we transplanted an FLDX-labelled piece of outer layer of one embryo onto a Cascade Blue (CB)-labelled inner layer of another and allowed to develop until stage 32 before labelling with a *foxa1* probe. *Foxa1*-labelled cells colocalise with CB cells and thus must originate from the inner layer (Fig. 2C). To check for the origin of goblet cells, we transplanted a piece of outer layer from one embryo (FLDX) onto the inner layer (MR) of another and reared until stage 32. The goblet cell marker, anti-Xeel shows colocalisation with FLDX, and hence the goblet cells must differentiate from the original outer layer cells (Fig. 2D).

The new cell type is small with large apical secretory vesicles

Using membrane-GFP and co-staining with markers for ciliated cells, ionocytes and goblet cells, we were able to determine the distinct morphology of these cells. This new cell type is small in size compared with its neighbours but contains large apical openings at the surface, evident with mGFP staining and by scanning electron microscopy (SEM; Fig. 3). The SEM image shows 'pores' (average diameter of 1.3±0.09 µm) on the surface of this cell type, which are likely to correspond to vesicles that have opened out to release their content (arrow highlights possible secretory material on the surface). Images obtained by transmission electron microscopy (TEM; Fig. 3B), showed an abundance of large vesicles at the apical membrane. Other vesicles, which are presumably immature, were evident deeper within the cell (yellow arrow). Magnification of the apical vesicles showed that they contain material with a dark, presumably dense, core surrounded by lighter material. A comparison with earlier studies of the *X. laevis* embryonic epidermis showed that these cells have been described by their morphology before (Hayes et al., 2007; Montorzi et al., 2000). Owing to their size and apparent

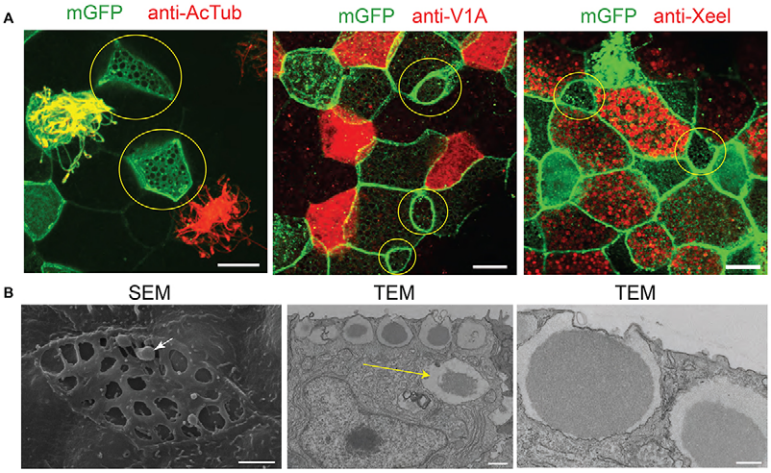

Fig. 3. Small cells with large vesicles containing secretory material. (A) Small cells (yellow circles) are not labelled by markers for ciliated cells (anti-AcTub), ionocytes (anti-V1a) or goblet cells (anti-Xeel). Membranes are marked with membrane GFP (mGFP). (B) SEM shows small cells with large apical openings and secretory material highlighted with an arrow. Sections imaged by TEM show vesicles at the apical membrane containing a dark core surrounded by lighter material. Highlighted with a yellow arrow is a vesicle deeper within the cytoplasm that may represent an immature vesicle. Scale bars: in A, 10 µm; in B, 2 µm (SEM), 1 µm (TEM, low magnification) and 0.5 µm (TEM, high magnification).

Development (2014) doi:10.1242/dev.102426

function, these cells were defined as small secretory cells (SSCs), a nomenclature retained here.

SSCs contain a number of different proteins including glycoproteins

The mRNA for inositol trisphosphate kinase b (*itpkb*), an enzyme that catalyses the conversion of IP_3 to IP_4 and is involved in calcium signalling,, is known to have a scattered, punctate epidermal expression pattern in *Xenopus* (Soto et al., 2013) and we confirmed this here (Fig. 4A). To see if *itpkb* is expressed in SSCs, we tested for colocalisation with *foxa1* by double *in situ* hybridisation and found complete overlap (Fig. 4B). Like *foxa1*, *itpkb* did not colocalise with markers for the other cell types (supplementary material Fig. S2). An antibody generated against Itpkb showed localisation in or around the secretory vesicles of the SSCs (Fig. 4C). The material in these vesicles was also recognised by peanut agglutinin (PNA), a lectin that binds the carbohydrate sequence Gal-β(1-3)-GalNAc (Fig. 4D,E). PNA was originally shown to bind to material in the epidermis of *X. laevis* (Slack, 1985); however, the cell types that secrete it were not defined. Here, we show that they are *foxa1*-expressing cells (Fig. 4D). PNA also recognised material in the vesicles of goblet cells, but at a much lower level than the SSCs (Fig. 4E, yellow arrow). In addition to the epidermal staining, PNA stained material secreted from the cement gland, which is also positive for a mucin, *muc5e* (supplementary material Fig. S3).

Another carbohydrate epitope, HNK-1 (HSO_3-3GlcAβ1-3Galβ1-4GlcNAc), also showed staining in a subset of epidermal cells in a previous study, but again the cell type was not properly defined (Somasekhar and Nordlander, 1997). Using a monoclonal antibody we found some vesicles in SSCs were highly positive for HNK-1 (Fig. 4F). PNA and HNK-1 tend to be found in different vesicles (Fig. 4G). However, other cells showed some colocalisation between the two markers (data not shown). Therefore, it is difficult to say at this stage if they represent distinct molecular species or perhaps, different stages of maturation.

Foxa1 is a regulator of SSC development

By analogy to the regulation of ionocytes by Foxi1 (Dubaissi and Papalopulu, 2011) and ciliated cells by Foxj1 (Stubbs et al., 2008; Yu et al., 2008), we hypothesised that Foxa1 may have a role in the development of SSCs. To test this, we knocked down *foxa1* with a morpholino targeting the splice junction of the exon-1-intron 1 boundary (Fig. 5A). Using cell type-specific markers, we found that there was no change in the number of ciliated cells or goblet cells, but there was a large decrease in the number of SSCs (61% reduction; Fig. 5B). There was also a substantial increase in the number of ionocytes (46%), suggesting that these two cell types are somehow linked in their development.

It is possible that SSCs are not properly specified in *foxa1* morphants. Alternatively, they may be correctly specified but undergo selective cell death early on. To distinguish these possibilities we examined the number of TUNEL-positive cells, together with an SSC marker (*itpkb*), at late neurula (stage 21) and late tailbud stage (stage 33) of *foxa1* morphant embryos. There was some increase in epidermal cell death at late tailbud stages, but at early stages *itpkb* expression was significantly reduced, even though there was no increase in cell death (supplementary material Fig. S4). Thus, the decrease in the SSCs upon *foxa1* knockdown is not primarily due to cell death.

Overexpression of *foxa1* had the opposite effect in that it increased the number of SSCs (supplementary material Fig. S5A).

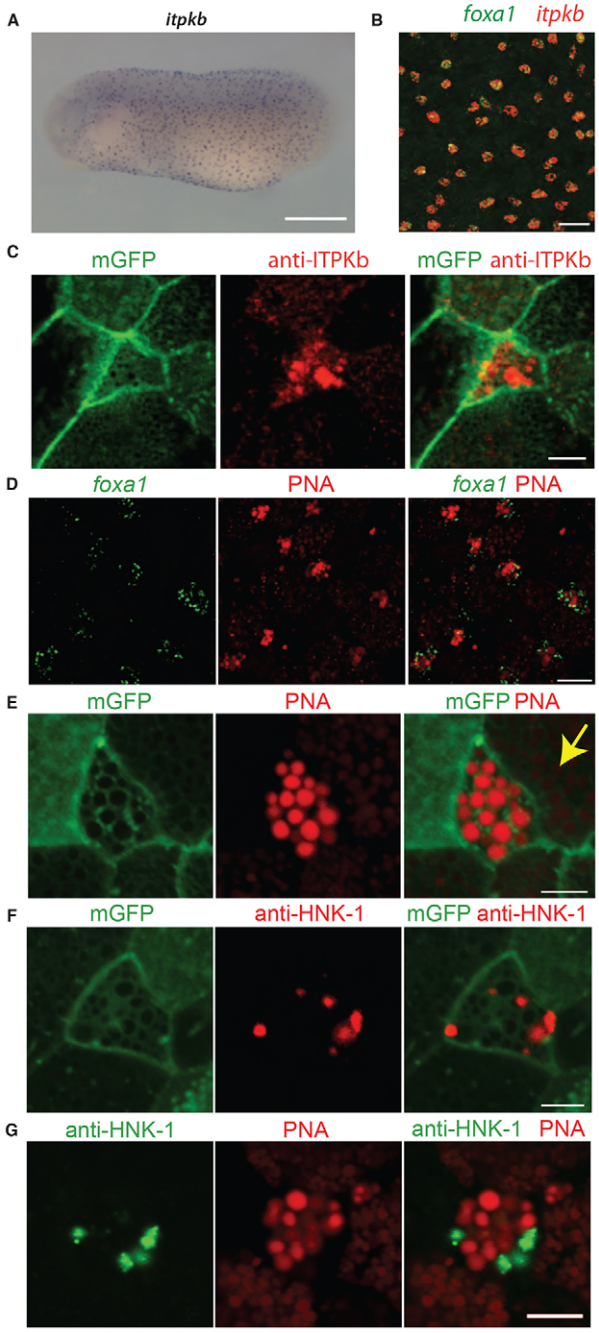

Fig. 4. Molecular profile of the new cell type. (A) *In situ* hybridisation using an antisense probe to the *itpkb* transcript reveals a scattered, punctate epidermal pattern. (B) Double fluorescence *in situ* hybridisation for *foxa1* and *itpkb* shows colocalisation of the two transcripts. (C) Antibody staining for Itpkb with mGFP shows localisation in the small cells with large apical vesicles. (D) PNA conjugated to Alexa Fluor-568 colocalises with *foxa1*. (E) PNA together with mGFP staining shows strong labelling of material in the large vesicles. Staining is also evident at a lower level in vesicles of goblet cells (yellow arrow). (F) Antibody staining to the carbohydrate epitope HNK-1 together with mGFP shows specific expression in the vesicles of the small cells. (G) Co-staining for HNK-1 and PNA shows that they are present in the same cell. Scale bars: 500 µm in A; 50 µm in B; 5 µm in C,E-G; 15 µm in D.

However, this was only evident at a low dose of overexpression (10 pg), whereas higher doses (>50 pg) resulted in the appearance of 'masses' of PNA-negative, smaller cells (supplementary material

Development (2014) doi:10.1242/dev.102426

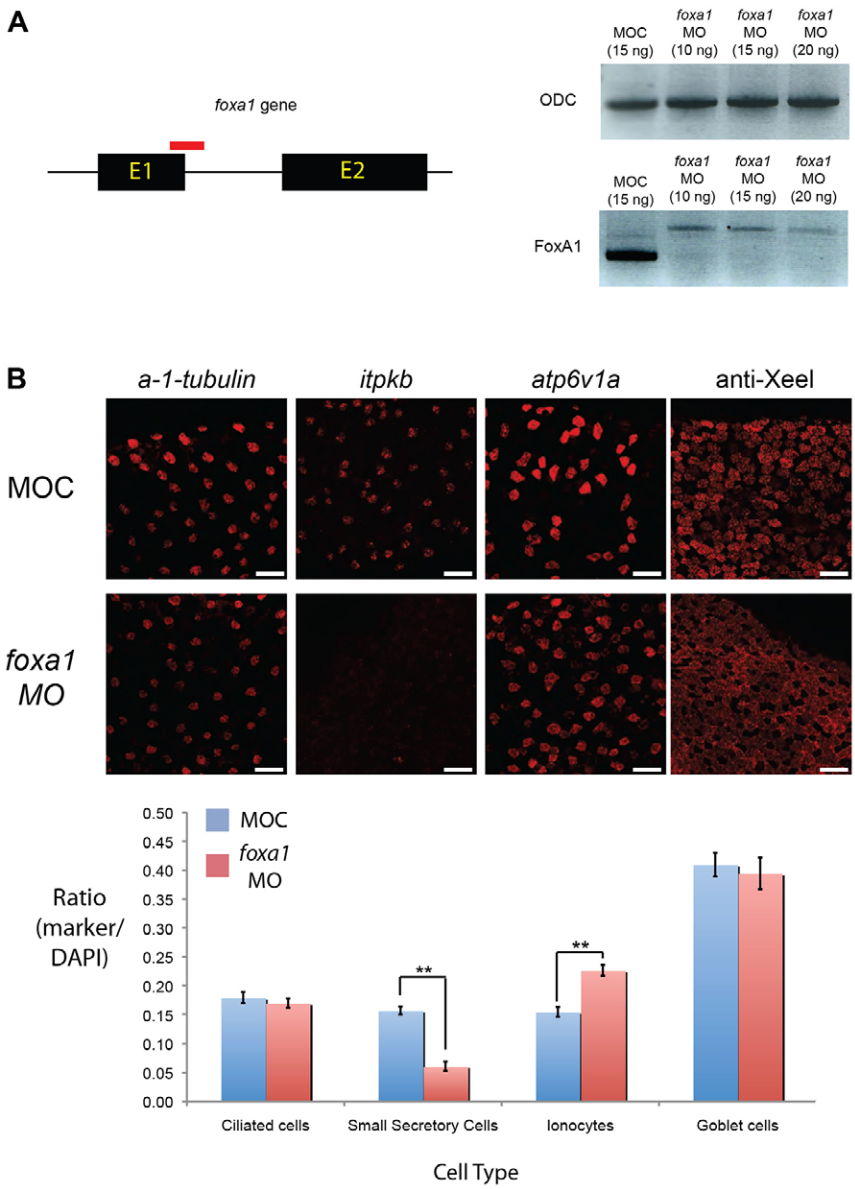

Fig. 5. FoxA1 is a regulator of SSC development. (A) The *foxa1* gene has two exons and one intron. An antisense morpholino oligo (red) was designed against the splice junction of exon 1 and intron 1. Loss of *foxa1* transcript is evident with *foxa1* MO compared with controls (MOC) by RT-PCR (using primers either side of the splice site), indicating knockdown of expression. A higher band was evident for the *foxa1* morphants, which is indicative of an unspliced transcript. There is no difference in the intensity of bands for the ubiquitously expressed gene *ornithine decarboxylase* (*ODC*). (B) Representative images of stage 32 embryos showing the frequency of each cell type after applying MOC or *foxa1* morpholino. Ciliated cells were marked by *α-1-tubulin*, SSCs by *itpkb*, ionocytes by *atp6v1a* and goblet cells by antibody to Xeel. The total number of cells in a defined area was determined by DAPI staining of nuclei and a ratio for each marker relative to the total number of cells was determined as shown in the chart. The mean ratio for ten embryos is shown for each sample. Error bars represent s.e.m. Student's *t*-test, $P<0.01$ (**). Scale bars: 50 µm.

Fig. S5B). This is consistent with previously suggested roles for FoxA1 in tumorigenesis (Nucera et al., 2009; Robinson et al., 2011; Yamaguchi et al., 2008).

Foxa1 morphants are susceptible to bacterial infection

When looking for the phenotypic consequences of *foxa1* knockdown, we noticed that embryos showed a marked tendency to die shortly after hatching from the vitelline membrane (Fig. 6A). The appearance of the embryo culture was reminiscent of bacterial infection, which occasionally happens, as we do not routinely supplement the medium with antibiotics. We therefore tested whether we can rescue the phenotype with antibiotics.

Embryos injected with control morpholino (MOC) showed excellent survival levels 2 days post-fertilisation (approximately stage 35-37), both with and without application of the broad-spectrum antibiotic, gentamicin (20 µg/ml; Fig. 6A). However, *foxa1* morphants, 2 days post-fertilisation, showed much reduced survival levels when cultured in 0.01× Marc's modified Ringer's (MMR) solution alone. Upon application of gentamicin, significant rescue of the survival rate was evident (Fig. 6A). Quantification of seven independent experiments (Fig. 6B) reveals that supplementing the media in which *foxa1* morphants were reared with antibiotic led to an increase in survival rate from ~27% to 80% ($P<0.01$). This compares to over 90% survival for control embryos with or without antibiotic.

To exclude the possibility that the phenotype is due to the increase in ionocytes that accompanies *foxa1* MO injections (see Fig. 5B), rather than the decrease in SSCs, we increased specifically the number of ionocytes by overexpression of *foxi1* (supplementary material Fig. S6A). This did not significantly affect the survival of the embryos (~90% survival) in three independent experiments and there was no effect by the addition of antibiotics (supplementary material Fig. S6B).

Loss of SSCs could cause the death of the embryos by having a major effect on the integrity of the epidermis. To answer this question we analysed control and morphants embryos by membrane GFP expression. We have found no obvious difference from the controls at late neurula and tadpole stages, although we did notice an increased tendency of some epidermal cells to round up at the later stages of analysis. However, cell-cell contact appeared normal (supplementary material Fig. S7).

Development (2014) doi:10.1242/dev.102426

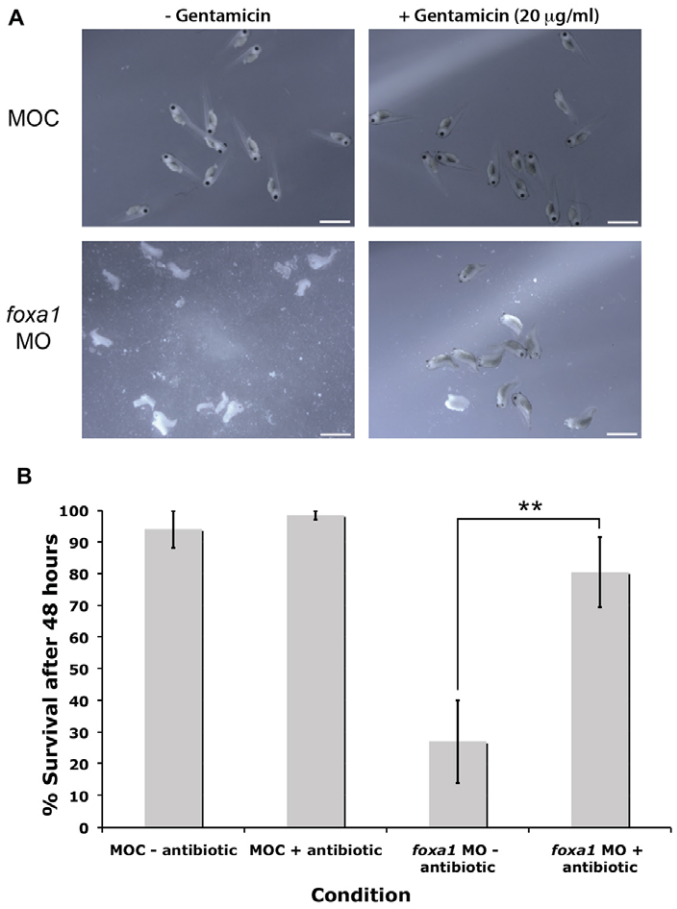

Fig. 6. Depletion of SSCs leaves embryos susceptible to infection. (A) Representative images showing embryo death following *foxa1* knockdown. Supplementing the media with the broad-spectrum antibiotic, gentamicin (20 µg/ml) leads to a greater level of survival. n=7 experiments. (B) Quantitation of the survival rate. Error bars represent s.e.m. Student's t-test, $^{**}P$<0.01. Scale bars: 2 mm.

SSCs secrete glycosylated and oligomeric material of high molecular weight

Given the protective action of the SSCs, we sought to identify components of the secretory material that are likely to account for this activity. As PNA recognises the material in the majority of the vesicles in the SSCs (Fig. 4E), we used PNA-HRP as a reagent for further investigation. Two PNA-positive species above 100 kDa were observed when the cement gland was present, but only a single species when the cement gland was removed (Fig. 7A, first four lanes). Comparing cement gland lysate and material aspirated directly from the epidermal surface confirmed that the species running lower in the gel corresponds to epidermal secretions and the material higher in the gel to the cement gland secretions (Fig. 7A, last two lanes). Comparing unreduced (–DTT) and reduced (+DTT) secretions from wild type without cement gland (WT – CG) embryos showed that the reduced samples migrate further in the gel (Fig. 7B). This indicates that the native PNA-positive material can form oligomers (and potentially polymers) through disulphide bonding. A comparison of secretions from *foxa1* morphants and controls showed a substantial decrease in the PNA-positive material corresponding to epidermal secretions (Fig. 7C, red arrow). There was little difference in the band corresponding to the cement gland material (Fig. 7C, blue arrow).

The apparent properties of high molecular weight, glycosylation and formation of oligomers through disulphide bonding is reminiscent of mucin glycoproteins. Mucins can be isolated based on their density, so to further enrich the PNA-positive material secreted from the epidermis we separated the samples using caesium chloride (CsCl) density gradient centrifugation. The chart in Fig. 7D shows a peak of PNA reactivity for fractions of density 1.3-1.4 g/ml, which is similar to the density of known mucins (Thornton et al., 1995). PNA-positive fractions were pooled and analysed by mass spectrometry, alongside samples taken before purification from embryos with and without cement gland, to identify any active components.

Mass spectrometry analysis of epidermal secretions identifies glycosylated and oligomeric molecules and other proteins involved in innate immunity

Table 1 summarises the top protein hits in mass spectrometry for the three sets of samples. One of the top hits in all three samples was a predicted protein, LOC100496483, which matched to a locus in the *X. tropicalis* genome (Hellsten et al., 2010). This protein appears most closely related (70% identity at the amino acid level) with a glycoprotein called Otogelin described in *X. laevis* (Hayes et al., 2007), so we called this protein Otogelin-like. As this protein gave the highest hit after purification by density gradient centrifugation and pooling PNA fractions, we postulated that this is the molecule recognised by PNA and secreted from the epidermis. To test this notion we generated an RNA probe to the *otogelin-like* transcript and observed its expression pattern at different stages of development (Fig. 7E). At stage 20, *otogelin-like* is expressed principally in the goblet cells, but by stage 32, there is strongest staining in the SSCs (supplementary material Fig. S8A) and a lower level in goblet cells and ionocytes, but not in the ciliated cells (supplementary material Fig. S8B-D). However, by stage 42 the expression of *otogelin-like* is almost completely confined to the SSCs. Figure 7F shows that the *otogelin-like* transcript has an overlapping expression pattern with PNA and this is particularly prominent in the SSCs.

To test the effect of *otogelin-like* depletion, we knocked it down using MO injections (Fig. 8A). Although in morphant embryos, there was a clear reduction in PNA staining (Fig. 8B) and an alteration in the morphology of secretory vesicles of goblet cells and SSCs by TEM (Fig. 8C), the viability of the embryos was normal until at least advanced tadpole stage (stage 42; data not shown). At that point, embryos showed swelling and eventually died, but this was not rescuable by antibiotics (data not shown). Together with earlier data, these results strongly suggest that the dense, oligomeric glycoprotein marked by PNA; secreted from the epidermis and reduced upon SSC depletion is the Otogelin-like species. However, knockdown of *otogelin-like* alone is not sufficient to phenocopy the *foxa1* morphants.

Of the other hits in mass spectrometry, the $IgGF_c\gamma$ binding protein (Fcgbp) was also found in the purified samples, which is interesting because it has been identified previously in intestinal mucus samples (Johansson et al., 2009). One predicted mucin, Muc5e, was identified but only in the WT+CG sample, indicating that it is secreted from the cement gland, which we confirmed by *in situ* hybridisation for *muc5e* (supplementary material Fig. S3B). Other interesting proteins present in the material before purification include two complement factors as well as the glycolipoproteins, vitellogenin and apolipoprotein B, which are implicated in innate immunity (Peterson et al., 2008; Zhang et al., 2011). It remains to be seen whether any of these candidates are secreted from epidermal cells, in particular the SSCs, and whether they contribute to innate immunity.

Development (2014) doi:10.1242/dev.102426

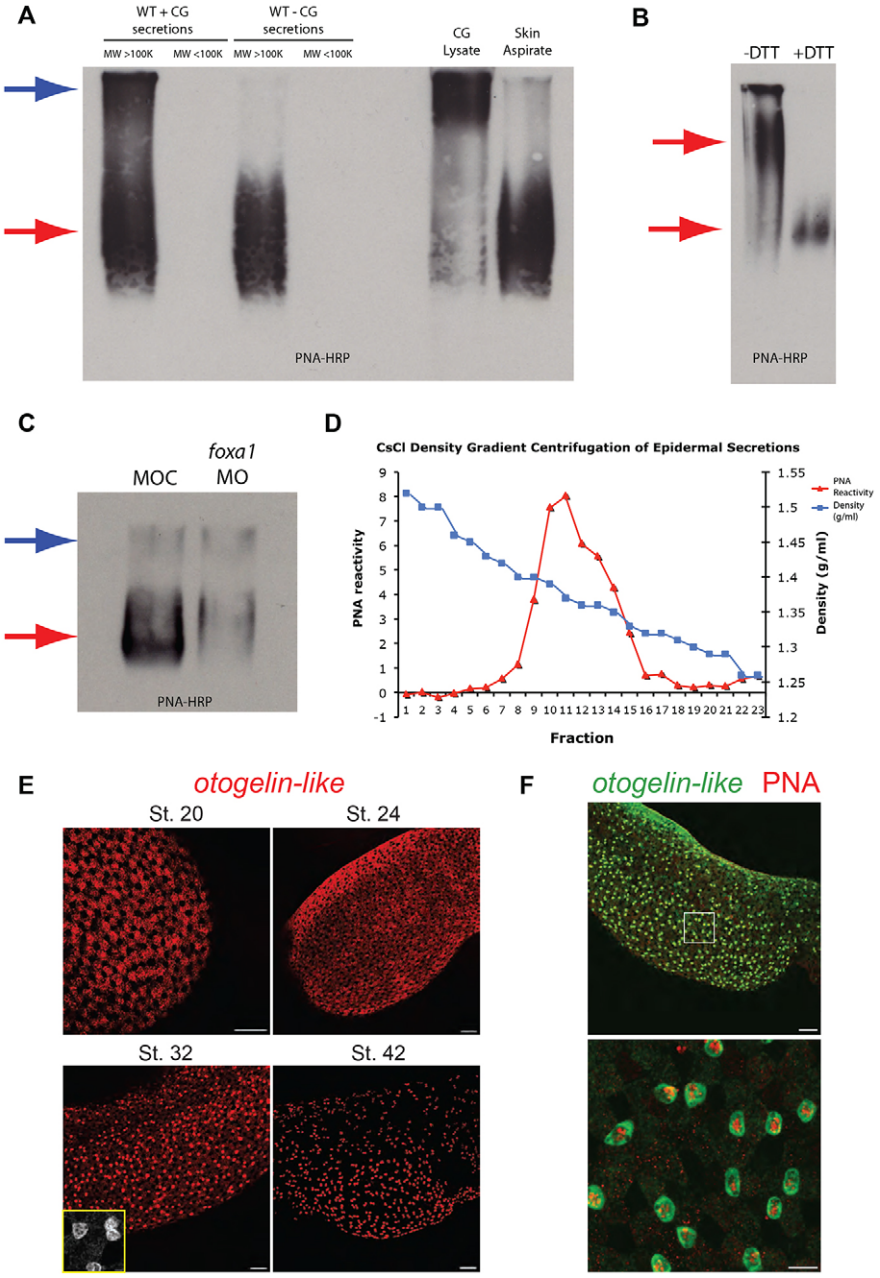

Fig. 7. SSCs secrete mucin-like molecule(s). (A) Lectin blot for PNA conjugated to horseradish peroxidase (PNA-HRP) of an agarose gel loaded with samples (reduced and alkylated). Secretions from wild-type embryos with cement gland (WT + CG), put through a filter to remove species with molecular weight lower than 100 kDa, shows two bands positive for PNA (blue and red arrows). For secretions from wild-type embryos with cement gland excised (WT – CG), there is only a single band evident (red arrow). Cement gland lysate alone gave predominantly the upper band, whereas aspirating directly from the skin gave predominantly the lower band. (B) Lectin blot for PNA-HRP of unreduced (–DTT) and reduced (+DTT) samples taken from secretions of wild-type embryos with cement gland removed. Reduced samples migrate much further in the gel. (C) Lectin blot for PNA-HRP comparing levels of PNA positive material secreted into the media in control and *foxa1* morpholino-injected embryos. There is a clear reduction in the lower band (red arrow), whereas the upper band (blue arrow) is of a similar level. (D) Chart showing results of CsCl density gradient centrifugation on samples obtained from the media of embryos with cement gland excised. Fractions of decreasing density were harvested and tested for PNA-reactivity in slot blots. Intensity measurements for PNA reactivity were recorded for each fraction and plotted as shown. (E) Timecourse of *otogelin-like* mRNA *in situ* hybridisation shows epidermal staining at four stages. There is strong staining in the SSCs at stage 32 (zoom, inset). (F) *Otogelin-like* (green) *in situ* hybridisation combined with PNA-Alexa-568 (red) staining, at stage 32, shows colocalisation in SSCs and goblet cells (at a lower level). Lower image is a magnification of the area in the box of the upper image. Scale bars: in E, 100 µm and 10 µm (stage 32 image, inset); in F, 100 µm (upper) and 20 µm (lower).

DISCUSSION

Using a combination of markers for the known epidermal cell types, new markers and ultrastructural analyses we have characterised a new cell type, the SSCs, in the *Xenopus* larval epidermis. With the characterisation of these secretory cells, all the cell types in the epidermis up to tadpole stages are accounted for. This is an important step in being able to fully utilise this system as a simple model to study the development and function of mucociliary epithelia and the interactions between cell types.

There has been some confusion in the literature as to the true identity of these cells. The fact that they are nonciliated, undergo an intercalation event and have a scattered epidermal distribution had led many, including ourselves, to assume that these cells are ionocytes (Dubaissi and Papalopulu, 2011; Quigley et al., 2011). Indeed, many of the gene markers for ionocytes and SSCs have been grouped together as being part of one cell type (Hayes et al., 2007). Our current study addresses this issue and shows that the SSCs are indeed a distinct cell type.

The transcription factor Foxa1 was found to be integral for the development of the SSCs. It is of note that this same transcription factor has been shown to be crucial in the development of numerous secretory cell types in mammals, including goblet cells and clara cells in the lung, and enteroendocrine cells in the gut (Besnard et al., 2004; Gao et al., 2010; Ye and Kaestner, 2009). In addition, Foxa1 has also been shown to directly transactivate expression of mucin genes (Jonckheere et al., 2007; van der Sluis et al., 2008). Together with our results, these findings suggest an evolutionarily conserved role of FoxA1 genes in regulating secretory cell fate in epithelial tissues.

Embryos that develop without SSCs, achieved by knocking down Foxa1, die around hatching, at a time that is coincident with SSC intercalation into the outer layer. We were able to rescue embryos

Development (2014) doi:10.1242/dev.102426

Table 1. *Xenopus* mass spec hits for protein in different samples

			Increased purification		
Accession	Mass (Da)	Description	WT+CG	WT-CG	WT-CG purified
VITEL6	202,707	Vitellogenin B1	57	55	0
F6W4K0	214,097	Vitellogenin A2	55	47	0
XP_002938567.1*	275,734	Otogelin-like (LOC100496483)	29	34	22
MUC5E‡	520,668	Muc5e	22	0	0
B5DEE0	189,095	Complement component C3	28	18	2
F6Z8Q2	500,791	Similar to apolipoprotein B-10	34	32	0
F7D692	217,975	Similar to Fcgbp	13	15	10
F7D002	610,692	Similar to Fcgbp	29	23	0
B0BMH7	47,776	Enolase 1	4	10	0
B0JZ32	67,837	Complement component C9	4	13	0
F6TCT8	164,583	Similar to α2 macroglobulin	7	10	0
F6YTJ1	226,504	Similar to myosin 9	3	10	0
F7D3F1	275,864	Similar to fibronectin	7	10	0

Proteins with 10 or more significant peptides (final three columns) are shown for each sample. 'WT-CG purified' represents secretions separated by density and pooling of PNA fractions. The hits for keratin and albumin are not shown. The number of significant peptides is shown. VITEL6 is a sequence for vitellogenin B1, which we added to our in-house mass spec database and is predicted from JGI. The full list of mass spec results for these three samples are shown in supplementary material Table S1.

*Alternative GenBank accession number is XP_004916622.1, which is a partial protein sequence.

‡Muc5e is a predicted protein identified in a genome-wide search for mucins (Lang et al., 2007).

from dying by the addition of antibiotics into the media, indicating that these cells provide a first line of defence against infection. We suggest that there are at least three ways by which SSCs may protect the embryo from infection.

First, SSCs may protect the epidermis from invasion by producing a mucus layer, which can trap bacteria and other particulate material and exclude its entry to the underlying epithelium. The major structural components of mucus are large, polymeric gel-forming glycoproteins called mucins (Thornton et al., 2008). Our EM data showed that the vesicles of SSCs contain dense material that visually resemble mucins in mammalian goblet cells (Wang et al., 2009). However, our extensive analysis of secretions did not identify any of the predicted mucins in the *X. tropicalis* genome, despite the fact that there are at least 25 (Lang et al., 2007). Indeed, as far as we are aware, the only embryonic mucin with known expression in *Xenopus* is our identification of Muc5e, which is produced by the cement gland. This is in contrast to the adult frog skin, where putative mucins have been identified in subdermal mucous glands and are thought to be secreted onto the surface of the skin (Hauser and Hoffmann, 1992; Schumacher et al., 1994).

Our screen did, however, identify another glycoprotein, Otogelin-like, which has characteristics of mucins. The otogelins are evolutionarily related to mucins, with both containing von Willebrand factor (vWF) domains and cysteine knot domains that facilitate disulphide bonding of monomers to generate large polymers (Lang et al., 2007). Otogelin has been identified in fibre-like structures in the acellular membranes of the inner ear in mammals including humans (Cohen-Salmon et al., 1997; Cohen-Salmon et al., 1999), and mutations in the *OTOG* gene can result in deafness (Schraders et al., 2012). The fact that Otogelin-like is glycosylated and able to form oligomers suggests that it is capable of forming the matrix of a mucus-like barrier over the surface of the embryo. We suggest that the Otogelin-like protein can undergo massive expansion once it is secreted to form a layer over the surface, just like mucins do (Kesimer et al., 2010). However, our knockdown experiments suggest that this Otogelin-like protein is not sufficient on its own to mediate anti-microbial defence of the epidermis and that there are likely to be other secreted molecules. Indeed, our EM analysis shows that some secretory material (of unknown identity) remains in the SSCs, even once Otogelin-like is knocked down (Fig. 8C).

Identification of the IgGFcγ-binding protein (FCGBP) is also interesting in terms of the generation of a mucus layer because it has been found to be covalently associated with the mucin Muc2 in the intestines of mice (Johansson et al., 2009). It also has many vWF domains, and has been postulated to cross-link mucins, adding stability to the mucus layer. It has also been shown to interact with other molecules in mucus, including the trefoil factors (Albert et al., 2010). Thus, FCGBP could also contribute to a mucus layer on the surface of the tadpole skin, although further tests are needed to confirm this.

A second possible way in which SSCs could provide protection against infection is to secrete innate defence and anti-infective molecules onto the surface. Adult frogs are known to secrete a potent cocktail of antimicrobial peptides (AMPs) onto the skin, including the magainins, from subdermal granular glands (Soravia et al., 1988; Zasloff, 1987). However, these AMPs have never been isolated in tadpoles before metamorphosis despite several attempts to do so (Zasloff, 2009). So how do the tadpoles protect themselves? Candidates in our mass spectrometry screen may give some clues. Some of our top hits were for the glycolipoproteins vitellogenin and apolipoprotein B. Vitellogenin is most commonly known as an egg yolk precursor protein that provides the energy source for developing embryos (Jorgensen et al., 2009). However, it has also been shown to have additional roles in innate immunity (Zhang et al., 2011). It has active antibacterial activity as well as the ability to recognise bacterial structures and promote phagocytosis (Li et al., 2008; Tong et al., 2010). Vitellogenin has also been identified as an antimicrobial agent in fish mucus (Meucci and Arukwe, 2005; Shi et al., 2006). Meanwhile, apolipoprotein B has been shown to antagonise and inhibit expression of invasive genes by *Staphylococcus aureus* and mice deficient for apolipoprotein B are more susceptible to infection (Peterson et al., 2008). The identification of the complement proteins, C3 and C9, in our mass spectrometry analysis is also of note because the complement cascade is a well-known innate defence system (Dunkelberger and Song, 2010; Janssen et al., 2005). Perhaps some of these molecules are secreted from the SSCs in addition to Otogelin-like. Thus, as

Development (2014) doi:10.1242/dev.102426

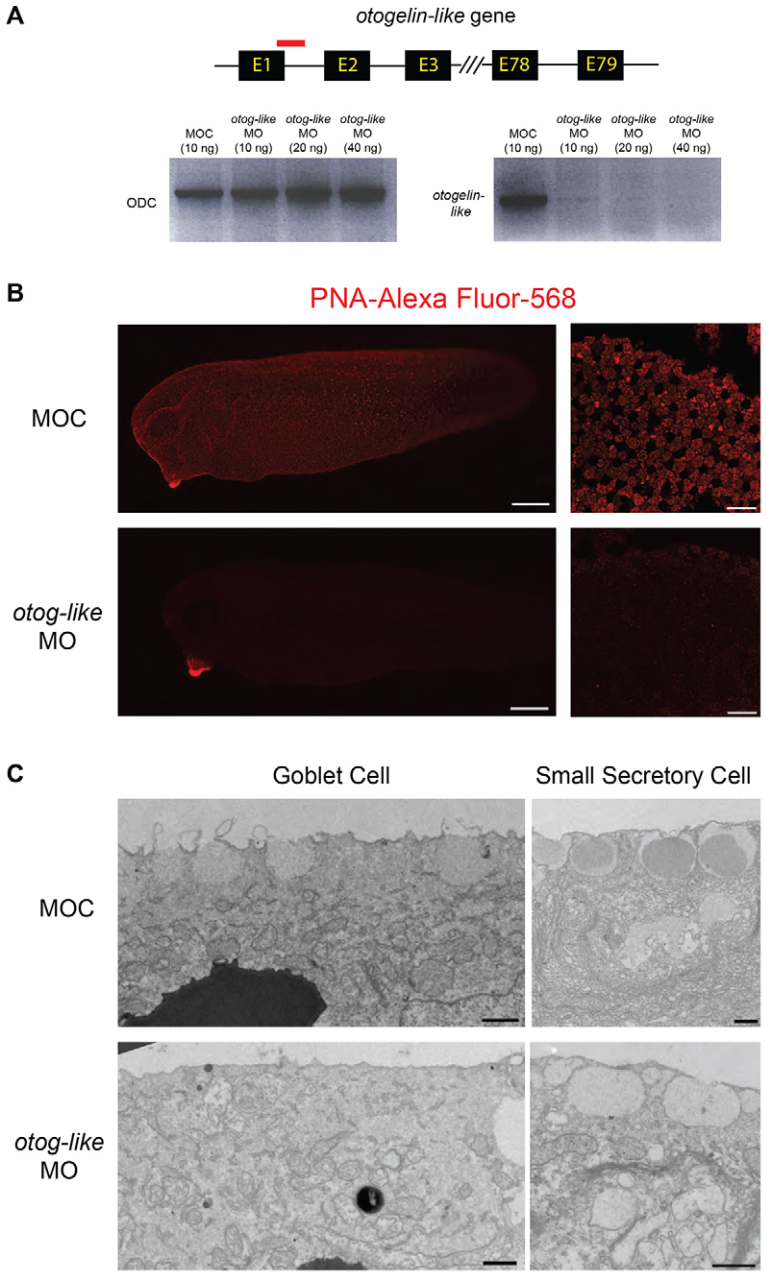

Fig. 8. Impact of *otogelin-like* knockdown on the epidermis. (A) The *otogelin-like* gene is predicted to have up to 79 exons and 78 introns. An antisense morpholino oligo (red) was designed against the splice junction of exon 1 and intron 1. Loss of *otogelin-like* transcript is evident with *otogelin-like* MO compared with controls (MOC) by RT-PCR, indicating knockdown of expression. There is little difference in the intensity of bands for the ubiquitously expressed gene, *ornithine decarboxylase* (*ODC*). (B) Comparison of PNA staining in otogelin-like morphants compared with controls (MOC). Right panels are higher magnification images of the flank epidermis. (C) TEM images of goblet cells and SSCs in controls (MOC) and *otog-like* MO treated embryos. Note absence of dark core in the vesicles of the SSCs. Scale bars: in B, 250 µm (left panels) and 50 µm (right panels); in C, 1 µm.

summarised in our model in Fig. 9, antimicrobial defence may be due to the combinatorial action of a number of molecules.

Finally, another contributor to the phenotype of enhanced susceptibility to infection could be an indirect effect of depleting SSCs on neighbouring cells. The accompanying paper by Walentek et al. describes how secretion of serotonin from the SSCs enhances the beating of cilia in adjacent ciliated cells (Walentek et al., 2014). In the absence of SSCs, the lack of serotonin could reduce ciliary beating and affect clearance of the mucus-like substance, leading to conditions where pathogens can thrive and infect the epidermis.

Through the initial characterisation of these cells, we have opened up the possibility for future studies into their role in innate immunity as well as other unexplored functions. The resemblance with the mucociliary epithelium of the respiratory tract is striking, and these similarities make the *Xenopus* larval skin a potentially very powerful model to study development, function and breakdown of these important epithelia.

MATERIALS AND METHODS

Morpholino design

All morpholinos were purchased from Gene Tools. The sequence of the *foxa1* splice morpholino is 5′-GGATTCCTTCTCTTACCTCCTGGGT-3′. The *otogelin-like* splice morpholino sequence is 5′-TAGAGTCATACA-TACCTCCATCATC-3′. The control morpholino has the sequence 5′-CCTCTTACCTCAGTTACAATTTATA-3′. Morpholinos were injected with a 15 ng dose at the one-cell stage unless otherwise stated.

Constructs and RNA generation

Constructs for generating probes were obtained from expressed sequence tag (EST) clones in the *Xenopus* full-length database (Gilchrist et al., 2004). The clone names were as follows: *atp6v1a* (TTpA014f09), *α-1-tubulin* (TNeu122k16), *otogelin-like* (THdA045k18), *foxa1* (TNeu062i17), *itpkb* (XM_002938844), *foxi1* (TNeu069d21), *foxj1* (TNeu058m03) and *muc5e* (TTbA069h06). The constructs were linearised and transcribed with T7 RNA polymerase (Promega) to generate antisense RNA probes. The probes were labelled with fluorescein isothiocyanate (FITC), digoxygenin (Dig) or

Development (2014) doi:10.1242/dev.102426

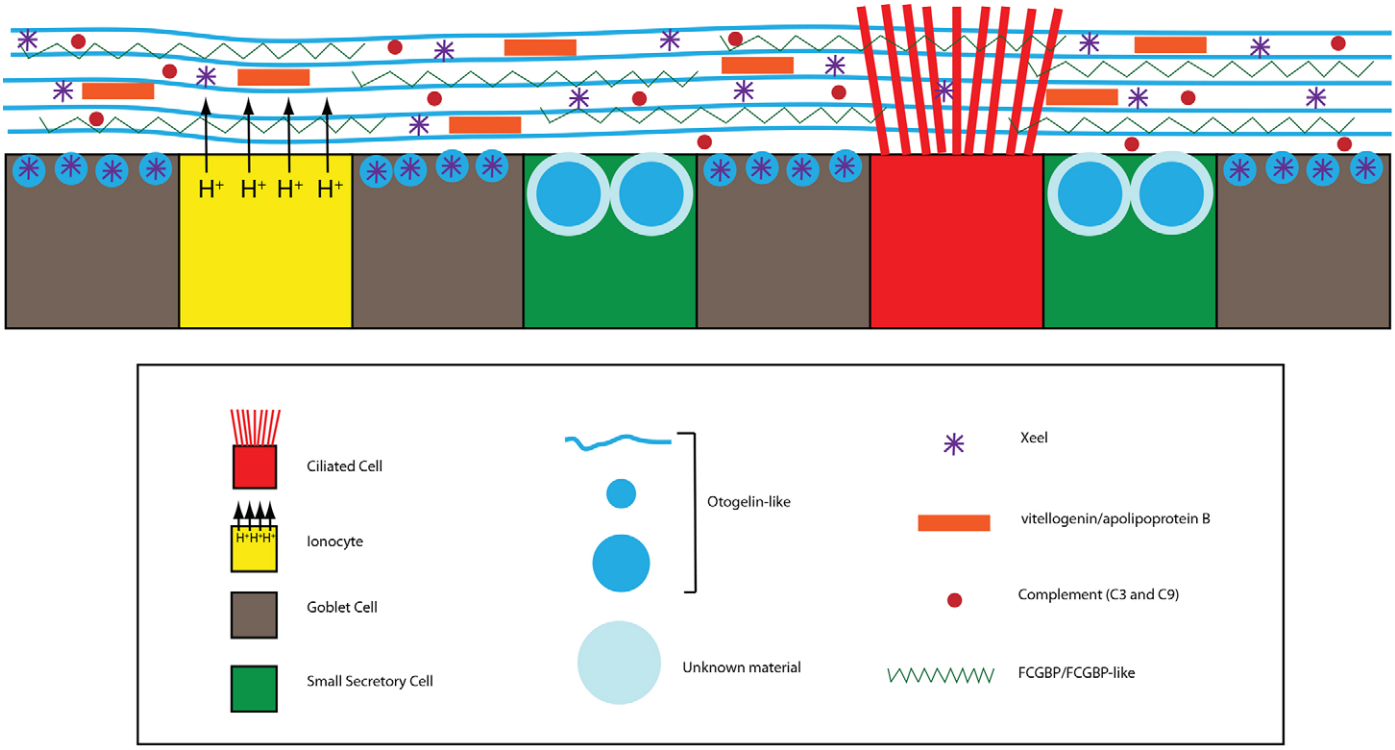

Fig. 9. Overview of *Xenopus* epidermal cell types and secretions. The epidermis of late tailbud/tadpole embryos has four cell types: ciliated cells, ionocytes, goblet cells and small secretory cells. Otogelin-like is a major secretory glycoprotein secreted from goblet cells and SSCs. Goblet cells also secrete the lectin, Xeel. SSCs also secrete another granular material in their vesicles that has yet to be identified. Other innate defence molecules found in secretions include vitellogenin, apolipoprotein b, complement factors (C3 and C9) and FCGBP/FCGBP-like proteins.

dinitrophenol (DNP). *In vitro* transcription was employed to generate *GAP43-GFP* mRNA from a pCS2-GAP43-GFP construct for injection into embryos and to mark membranes (Kim et al., 1998). The construct was linearised with *Not*I and transcribed with SP6 RNA polymerase (Promega).

Whole-mount chromogenic and fluorescence *in situ* hybridisation

Chromogenic *in situ* hybridisation was carried out as described (Harland, 1991). Multicolour fluorescence *in situ* hybridisation was performed using tyramide amplification after addition of probes and antibodies conjugated to horseradish peroxidase (Lea et al., 2012).

Immunofluorescence and lectin fluorescence

Immunofluorescence was largely carried out as described previously (Dubaissi and Papalopulu, 2011; Dubaissi et al., 2012). All primary antibodies for immunofluorescence were used at a dilution of 1:1000. Secondary antibodies (Invitrogen) conjugated to fluorophores were used at a dilution of 1:500. The following primary antibodies were used: mouse anti-acetylated α-tubulin (T7451; Sigma), rabbit anti-V1a (ST170; a gift from Shigeyasu Tanaka, Shizuoka University, Japan), mouse-anti-Xeel (a gift from Saburo Nagata, Japan's Women's University, Tokyo, Japan), mouse anti-HNK-1 antibody (C6680; Sigma), rabbit anti-GFP antibody (A-6455; Life Technologies) and a custom-made rabbit anti-Itpkb antibody (Cambridge Research Biochemicals, UK). The lectin, PNA conjugated to Alexa Fluor 568 (Life Technologies), was used at a dilution of 1:1000.

Epidermal transplantation

Embryos were injected with the fluorophores MR, FLDX or CB (all Invitrogen), at the eight-cell stage in two ventral blastomeres fated to become epidermal tissue. The embryos were reared in 0.01× MMR until gastrulation and then transferred to transplantation buffer [0.5× MMR, 1% Ficoll and 5 µg/ml gentamicin (Sigma)]. Tungsten wires were used to remove a section of outer layer epidermis from one set of fluorophore-injected embryos. A section of outer layer tissue from a different set of fluorophore-injected embryos was then transplanted onto the inner layer of the first set and the embryos were left for 2 hours to heal. The embryos were then transferred to post-transplantation buffer (0.1× MMR, 5 µg/ml gentamicin) and reared until stage 32, when they were fixed for analysis.

TUNEL staining

The TUNEL protocol on *Xenopus* embryos was performed largely as described previously (Hensey and Gautier, 1998). In summary, embryos were fixed in MEMFA and stored in methanol. Embryos were bleached (70% methanol, 10% H_2O_2, 5% formamide) to remove pigment and then rehydrated into PBS. Embryos were incubated in 150 U/ml terminal deoxynucleotidyltransferase (Invitrogen) and digoxygenin-dUTP (1:1000, Roche). Reaction was terminated with 1 mM EDTA in PBS. The normal *in situ* hybridisation protocol was then followed using anti-digoxygenin antibody conjugated to alkaline phosphatase and chromogenic reaction using nitro-blue tetrazolium chloride/5-bromo-4-chloro-3′-indolyphosphate p-toluidine salt (NBT/BCIP) as a substrate (Harland, 1991).

Collection of embryonic secretions

Embryos were reared in 0.01× MMR for 24 hours until stages 22-24 and then, if required, cement glands were removed with forceps in 0.01× MMR + gentamicin (10 µg/ml). Embryos were then reared until stage 35. To get enough material, 300 embryos were packed into a well containing 600 µl of media. The embryos were reared for 4 hours at room temperature with agitation every 20 minutes. Embryos were then anaesthetised with tricaine and the media removed for analysis of secretions. Material was also aspirated directly from the epidermis using glass Pasteur pipettes. Denaturants such as 6 M urea or 8 M guanidinium chloride were added to denature any proteins. If required, samples were reduced in 10 mM dithiothreitol (37°C for 1 hour) and alkylated in 25 mM iodoacetamide (30 minutes at room temperature in the dark). To concentrate the secretory material, the media samples were centrifuged through Vivaspin columns

(Sartorius Stedim Biotech) that trap material above a certain molecular weight. We used filters with a 100,000 MW cut-off so any material above this size was retained.

Agarose gel electrophoresis and PNA lectin blot

Agarose gels are used to separate high molecular weight and highly charged molecules such as mucins. Agarose gels were made at 1% (w/v) in tris-acetate-EDTA (TAE). Samples were loaded and electrophoresed at 65 V for 4-6 hours. After separation, proteins were vacuum blotted on to nitrocellulose membranes for 90 minutes in 4× SSC. PNA conjugated to horseradish peroxidase (PNA-HRP, Sigma) was applied to the membranes at a dilution of 1:1000 for two hours. The membranes were then washed four times for 5 minutes each in TBS-Tween, reacted with chemiluminescence reagents (Sigma), and exposed to photographic film (Kodak).

Caesium chloride density gradient centrifugation

Collected samples were separated by CsCl/4 M guanidinium chloride density gradient centrifugation (Thornton et al., 1999). The starting density was 1.4 g/ml and a Beckman Ti70 rotor was used to generate the gradient in an ultracentrifuge at 164,685 ***g*** for 68 hours at 15°C. Fractions (0.5 ml) were taken and assessed for PNA reactivity and density. Positive fractions were pooled, reduced and alkylated, and concentrated on Vivaspin columns before mass spectrometry.

Mass spectrometry

Samples were exchanged into 2 M urea (50 mM ammonium bicarbonate) using Vivaspin columns and digested overnight in trypsin (1 µg, Sigma). The tryptic peptides were purified using ZipTips (Millipore) and solubilised in 0.1% formic acid. Tryptic peptides were separated by reverse phase liquid chromatography (LC) and analysed by tandem mass spectrometry (LC-MS/MS) using a NanoAcquity LC (Waters, Manchester, UK) coupled to a LTQ Velos mass spectrometer (Thermo Fisher Scientific). MS/MS data were searched using Mascot 2.4 (Matrix Science, UK) software against a custom database consisting of the SWISSPROT database with additional predicted *Xenopus tropicalis*-specific mucin sequences (Lang et al., 2007). The parameters were as follows: Carbamidomethyl (C) as fixed modification, Oxidation (M) as variable modification, peptides mass tolerance of 1.2 Da, fragments mass tolerance 0.6 Da, 1 missed cleavage maximum.

Electron microscopy

SEM and TEM were performed according to standard protocols. For SEM, embryos were fixed in 2.5% glutaraldehyde in 0.1 M sodium cacodylate buffer (pH 7.2) and then postfixed in osmium tetroxide. Embryos were then critical point dried and sputter-coated with gold. Imaging was performed on an FEI Model Quanta 200 ESEM. For TEM, embryos were fixed overnight in 2% formaldehyde + 2% glutaraldehyde in 0.1 M cacodylate and then post-fixed in reduced osmium. The embryos were then put in 1% tannic acid and then 1% uranyl acetate, for 1 hour each. Samples were then dehydrated in ethanol and embedded in low viscosity resin. Sections of 70 nm were cut on a Reichert-Jung Ultracut E ultramicrotome and observed using an FEI Tecnai 12 electron microscope at 80 kV.

Acknowledgements

We thank staff in the EM facility in the Faculty of Life Sciences, University of Manchester, for their assistance, and the Wellcome Trust for equipment grant support to the EM facility; Aleksandr Mironov, Leslie Lockey and Patrick Hill for assistance with EM; Raphael Thuret for help with collection of samples and Bethan Powell for assistance with *in situ* hybridisation; Saburo Nagata and Shigeyasu Tanaka for donation of antibodies; Martin Blum for sharing data and reagents prior to publication; and Kristian Franze for some help in the early stages of analysis of the phenotype.

Competing interests

The authors declare no competing financial interests.

Author contributions

E.D., K.R., R.L., X.S. and S.N. performed the experiments. E.D., K.R., D.J.T. and N.P designed the experiments. The manuscript was written by E.D. and N.P., and edited by E.A., A.S. and D.J.T.

Funding

This work was supported by a Wellcome Trust Senior Research Fellowship [WT 090868Z/09/Z to N.P.]; a Wellcome Trust Institutional Strategic Support Fund grant [097820/Z/11/Z to N.P. and E.D.]; core funding to the Wellcome Trust Centre for Cell-Matrix Research [WT 088785/Z/09/Z]; and a Medical Research Council grant [G1000450 to D.J.T]. Deposited in PMC for immediate release.

Supplementary material

Supplementary material available online at
http://dev.biologists.org/lookup/suppl/doi:10.1242/dev.102426/-/DC1

References

Albert, T. K., Laubinger, W., Müller, S., Hanisch, F.-G., Kalinski, T., Meyer, F. and Hoffmann, W. (2010). Human intestinal TFF3 forms disulfide-linked heteromers with the mucus-associated FCGBP protein and is released by hydrogen sulfide. *J. Proteome Res.* **9**, 3108-3117.

Besnard, V., Wert, S. E., Hull, W. M. and Whitsett, J. A. (2004). Immunohistochemical localization of Foxa1 and Foxa2 in mouse embryos and adult tissues. *Gene Expr. Patterns* **5**, 193-208.

Billett, F. S. and Gould, R. P. (1971). Fine structural changes in the differentiating epidermis of Xenopus laevis embryos. *J. Anat.* **108**, 465-480.

Cohen-Salmon, M., El-Amraoui, A., Leibovici, M. and Petit, C. (1997). Otogelin: a glycoprotein specific to the acellular membranes of the inner ear. *Proc. Natl. Acad. Sci. USA* **94**, 14450-14455.

Cohen-Salmon, M., Mattei, M. G. and Petit, C. (1999). Mapping of the otogelin gene (OTGN) to mouse chromosome 7 and human chromosome 11p14.3: a candidate for human autosomal recessive nonsyndromic deafness DFNB18. *Mamm. Genome* **10**, 520-522.

Deblandre, G. A., Wettstein, D. A., Koyano-Nakagawa, N. and Kintner, C. (1999). A two-step mechanism generates the spacing pattern of the ciliated cells in the skin of Xenopus embryos. *Development* **126**, 4715-4728.

Drysdale, T. A. and Elinson, R. P. (1992). Cell migration and induction in the development of the surface ectodermal pattern of the Xenopus laevis tadpole. (Xenopus/ciliated cell/hatching gland/cement gland/ectodermal differentiation). *Dev. Growth Differ.* **34**, 51-59.

Dubaissi, E. and Papalopulu, N. (2011). Embryonic frog epidermis: a model for the study of cell-cell interactions in the development of mucociliary disease. *Dis. Model. Mech.* **4**, 179-192.

Dubaissi, E., Panagiotaki, N., Papalopulu, N. and Vize, P. D. (2012). Antibody development and use in chromogenic and fluorescent immunostaining. In *Xenopus Protocols* (ed. Hoppler, S. and Vize, P. D.), pp. 411-429. Totowa, NJ: Humana Press.

Dunkelberger, J. R. and Song, W.-C. (2010). Complement and its role in innate and adaptive immune responses. *Cell Res.* **20**, 34-50.

Engelhardt, J. F., Yankaskas, J. R., Ernst, S. A., Yang, Y., Marino, C. R., Boucher, R. C., Cohn, J. A. and Wilson, J. M. (1992). Submucosal glands are the predominant site of CFTR expression in the human bronchus. *Nat. Genet.* **2**, 240-248.

Gao, N., Le Lay, J., Qin, W., Doliba, N., Schug, J., Fox, A. J., Smirnova, O., Matschinsky, F. M. and Kaestner, K. H. (2010). Foxa1 and Foxa2 maintain the metabolic and secretory features of the mature beta-cell. *Mol. Endocrinol.* **24**, 1594-1604.

Garcia, M. A. S., Yang, N. and Quinton, P. M. (2009). Normal mouse intestinal mucus release requires cystic fibrosis transmembrane regulator-dependent bicarbonate secretion. *J. Clin. Invest.* **119**, 2613-2622.

Gilchrist, M. J., Zorn, A. M., Voigt, J., Smith, J. C., Papalopulu, N. and Amaya, E. (2004). Defining a large set of full-length clones from a Xenopus tropicalis EST project. *Dev. Biol.* **271**, 498-516.

Harland, R. M. (1991). In situ hybridization: an improved whole-mount method for Xenopus embryos. *Methods Cell Biol.* **36**, 685-695.

Hauser, F. and Hoffmann, W. (1992). P-domains as shuffled cysteine-rich modules in integumentary mucin C.1 (FIM-C.1) from Xenopus laevis. Polydispersity and genetic polymorphism. *J. Biol. Chem.* **267**, 24620-24624.

Hayes, J. M., Kim, S. K., Abitua, P. B., Park, T. J., Herrington, E. R., Kitayama, A., Grow, M. W., Ueno, N. and Wallingford, J. B. (2007). Identification of novel ciliogenesis factors using a new in vivo model for mucociliary epithelial development. *Dev. Biol.* **312**, 115-130.

Hellsten, U., Harland, R. M., Gilchrist, M. J., Hendrix, D., Jurka, J., Kapitonov, V., Ovcharenko, I., Putnam, N. H., Shu, S., Taher, L. et al. (2010). The genome of the Western clawed frog Xenopus tropicalis. *Science* **328**, 633-636.

Hensey, C. and Gautier, J. (1998). Programmed cell death during Xenopus development: a spatio-temporal analysis. *Dev. Biol.* **203**, 36-48.

Houtmeyers, E., Gosselink, R., Gayan-Ramirez, G. and Decramer, M. (1999). Regulation of mucociliary clearance in health and disease. *Eur. Respir. J.* **13**, 1177-1188.

Janssen, B. J. C., Huizinga, E. G., Raaijmakers, H. C. A., Roos, A., Daha, M. R., Nilsson-Ekdahl, K., Nilsson, B. and Gros, P. (2005). Structures of complement component C3 provide insights into the function and evolution of immunity. *Nature* **437**, 505-511.

Johansson, M. E. V., Thomsson, K. A. and Hansson, G. C. (2009). Proteomic analyses of the two mucus layers of the colon barrier reveal that their main component, the Muc2 mucin, is strongly bound to the Fcgbp protein. *J. Proteome Res.* **8**, 3549-3557.

Jonckheere, N., Vincent, A., Perrais, M., Ducourouble, M.-P., Male, A. K., Aubert, J.-P., Pigny, P., Carraway, K. L., Freund, J.-N., Renes, I. B. et al. (2007). The

human mucin MUC4 is transcriptionally regulated by caudal-related homeobox, hepatocyte nuclear factors, forkhead box A, and GATA endodermal transcription factors in epithelial cancer cells. *J. Biol. Chem.* **282**, 22638-22650.
Jorgensen, P., Steen, J. A. J., Steen, H. and Kirschner, M. W. (2009). The mechanism and pattern of yolk consumption provide insight into embryonic nutrition in Xenopus. *Development* **136**, 1539-1548.
Kesimer, M., Makhov, A. M., Griffith, J. D., Verdugo, P. and Sheehan, J. K. (2010). Unpacking a gel-forming mucin: a view of MUC5B organization after granular release. *Am. J. Physiol.* **298**, L15-L22.
Kim, S. H., Yamamoto, A., Bouwmeester, T., Agius, E. and Robertis, E. M. (1998). The role of paraxial protocadherin in selective adhesion and cell movements of the mesoderm during Xenopus gastrulation. *Development* **125**, 4681-4690.
Kim, S. K., Shindo, A., Park, T. J., Oh, E. C., Ghosh, S., Gray, R. S., Lewis, R. A., Johnson, C. A., Attie-Bittach, T., Katsanis, N. et al. (2010). Planar cell polarity acts through septins to control collective cell movement and ciliogenesis. *Science* **329**, 1337-1340.
Lang, T., Hansson, G. C. and Samuelsson, T. (2007). Gel-forming mucins appeared early in metazoan evolution. *Proc. Natl. Acad. Sci. USA* **104**, 16209-16214.
Lea, R., Bonev, B., Dubaissi, E., Vize, P. D. and Papalopulu, N. (2012). Multicolor fluorescent in situ mRNA hybridization (FISH) on whole mounts and sections. In *Xenopus Protocols* (ed. Hoppler, S. and Vize, P. D.), pp. 431-444. Totowa, NJ: Humana Press.
Li, Z., Zhang, S. and Liu, Q. (2008). Vitellogenin functions as a multivalent pattern recognition receptor with an opsonic activity. *PLoS ONE* **3**, e1940.
Loffing, J., Moyer, B. D., Reynolds, D., Shmukler, B. E., Alper, S. L. and Stanton, B. A. (2000). Functional and molecular characterization of an anion exchanger in airway serous epithelial cells. *Am. J. Physiol.* **279**, C1016-C1023.
Meucci, V. and Arukwe, A. (2005). Detection of vitellogenin and zona radiata protein expressions in surface mucus of immature juvenile Atlantic salmon (Salmo salar) exposed to waterborne nonylphenol. *Aquat. Toxicol.* **73**, 1-10.
Mitchell, B., Jacobs, R., Li, J., Chien, S. and Kintner, C. (2007). A positive feedback mechanism governs the polarity and motion of motile cilia. *Nature* **447**, 97-101.
Montorzi, M., Burgos, M. H. and Falchuk, K. H. (2000). Xenopus laevis embryo development: arrest of epidermal cell differentiation by the chelating agent 1,10-phenanthroline. *Mol. Reprod. Dev.* **55**, 75-82.
Nagata, S., Nakanishi, M., Nanba, R. and Fujita, N. (2003). Developmental expression of XEEL, a novel molecule of the Xenopus oocyte cortical granule lectin family. *Dev. Genes Evol.* **213**, 368-370.
Nishikawa, S. and Sasaki, F. (1993). Secretion of chondroitin sulfate from embryonic epidermal cells in Xenopus laevis. *J. Histochem. Cytochem.* **41**, 1373-1381.
Nucera, C., Eeckhoute, J., Finn, S., Carroll, J. S., Ligon, A. H., Priolo, C., Fadda, G., Toner, M., Sheils, O., Attard, M. et al. (2009). FOXA1 is a potential oncogene in anaplastic thyroid carcinoma. *Clin. Cancer Res.* **15**, 3680-3689.
Park, T. J., Mitchell, B. J., Abitua, P. B., Kintner, C. and Wallingford, J. B. (2008). Dishevelled controls apical docking and planar polarization of basal bodies in ciliated epithelial cells. *Nat. Genet.* **40**, 871-879.
Peterson, M. M., Mack, J. L., Hall, P. R., Alsup, A. A., Alexander, S. M., Sully, E. K., Sawires, Y. S., Cheung, A. L., Otto, M. and Gresham, H. D. (2008). Apolipoprotein B Is an innate barrier against invasive Staphylococcus aureus infection. *Cell Host Microbe* **4**, 555-566.
Quigley, I. K., Stubbs, J. L. and Kintner, C. (2011). Specification of ion transport cells in the Xenopus larval skin. *Development* **138**, 705-714.
Robinson, J. L. L., Macarthur, S., Ross-Innes, C. S., Tilley, W. D., Neal, D. E., Mills, I. G. and Carroll, J. S. (2011). Androgen receptor driven transcription in molecular apocrine breast cancer is mediated by FoxA1. *EMBO J.* **30**, 3019-3027.
Schraders, M., Ruiz-Palmero, L., Kalay, E., Oostrik, J., del Castillo, F. J., Sezgin, O., Beynon, A. J., Strom, T. M., Pennings, R. J. E., Seco, C. Z. et al. (2012). Mutations of the gene encoding otogelin are a cause of autosomal-recessive nonsyndromic moderate hearing impairment. *Am. J. Hum. Genet.* **91**, 883-889.
Schumacher, U., Adam, E., Hauser, F., Probst, J. C. and Hoffmann, W. (1994). Molecular anatomy of a skin gland: histochemical and biochemical investigations on the mucous glands of Xenopus laevis. *J. Histochem. Cytochem.* **42**, 57-65.
Shi, X., Zhang, S. and Pang, Q. (2006). Vitellogenin is a novel player in defense reactions. *Fish Shellfish Immunol.* **20**, 769-772.
Simons, M., Gault, W. J., Gotthardt, D., Rohatgi, R., Klein, T. J., Shao, Y., Lee, H.-J., Wu, A.-L., Fang, Y., Satlin, L. M. et al. (2009). Electrochemical cues regulate assembly of the Frizzled/Dishevelled complex at the plasma membrane during planar epithelial polarization. *Nat. Cell Biol.* **11**, 286-294.
Slack, J. M. W. (1985). Peanut lectin receptors in the early amphibian embryo: regional markers for the study of embryonic induction. *Cell* **41**, 237-247.
Somasekhar, T. and Nordlander, R. H. (1997). Selective early innervation of a subset of epidermal cells in Xenopus may be mediated by chondroitin sulfate proteoglycans. *Brain Res. Dev. Brain Res.* **99**, 208-215.
Soravia, E., Martini, G. and Zasloff, M. (1988). Antimicrobial properties of peptides from Xenopus granular gland secretions. *FEBS Lett.* **228**, 337-340.
Soto, X., Li, J., Lea, R., Dubaissi, E., Papalopulu, N. and Amaya, E. (2013). Inositol kinase and its product accelerate wound healing by modulating calcium levels, Rho GTPases, and F-actin assembly. *Proc. Natl. Acad. Sci. USA* **110**, 11029-11034.
Stubbs, J. L., Oishi, I., Izpisúa Belmonte, J. C. and Kintner, C. (2008). The forkhead protein Foxj1 specifies node-like cilia in Xenopus and zebrafish embryos. *Nat. Genet.* **40**, 1454-1460.
Stubbs, J. L., Vladar, E. K., Axelrod, J. D. and Kintner, C. (2012). Multicilin promotes centriole assembly and ciliogenesis during multiciliate cell differentiation. *Nat. Cell Biol.* **14**, 140-147.
Thornton, D. J., Howard, M., Devine, P. L. and Sheehan, J. K. (1995). Methods for separation and deglycosylation of mucin subunits. *Anal. Biochem.* **227**, 162-167.
Thornton, D. J., Khan, N., Mehrotra, R., Howard, M., Veerman, E., Packer, N. H. and Sheehan, J. K. (1999). Salivary mucin MG1 is comprised almost entirely of different glycosylated forms of the MUC5B gene product. *Glycobiology* **9**, 293-302.
Thornton, D. J., Rousseau, K. and McGuckin, M. A. (2008). Structure and function of the polymeric mucins in airways mucus. *Annu. Rev. Physiol.* **70**, 459-486.
Tong, Z., Li, L., Pawar, R. and Zhang, S. (2010). Vitellogenin is an acute phase protein with bacterial-binding and inhibiting activities. *Immunobiology* **215**, 898-902.
van der Sluis, M., Vincent, A., Bouma, J., Korteland-Van Male, A., van Goudoever, J. B., Renes, I. B. and Van Seuningen, I. (2008). Forkhead box transcription factors Foxa1 and Foxa2 are important regulators of Muc2 mucin expression in intestinal epithelial cells. *Biochem. Biophys. Res. Commun.* **369**, 1108-1113.
Walentek, P., Bogusch, S., Thumberger, T., Vick, P., Dubaissi, E., Beyer, T., Blum, M. and Schweickert, A. (2014). A novel serotonin-secreting cell type regulates ciliary motility in the mucociliary epidermis of Xenopus tadpoles. *Development* **141**, 1525-1532.
Wang, I.-J., Yu, C.-J. and Hu, F.-R. (2009). Alteration of ocular surface mucins in MUC5AC-DTA transgenic mice. *Mol. Vis.* **15**, 108-119.
Yamaguchi, N., Ito, E., Azuma, S., Honma, R., Yanagisawa, Y., Nishikawa, A., Kawamura, M., Imai, J., Tatsuta, K., Inoue, J. et al. (2008). FoxA1 as a lineage-specific oncogene in luminal type breast cancer. *Biochem. Biophys. Res. Commun.* **365**, 711-717.
Ye, D. Z. and Kaestner, K. H. (2009). Foxa1 and Foxa2 control the differentiation of goblet and enteroendocrine L- and D-cells in mice. *Gastroenterology* **137**, 2052-2062.
Yu, X., Ng, C. P., Habacher, H. and Roy, S. (2008). Foxj1 transcription factors are master regulators of the motile ciliogenic program. *Nat. Genet.* **40**, 1445-1453.
Zasloff, M. (1987). Magainins, a class of antimicrobial peptides from Xenopus skin: isolation, characterization of two active forms, and partial cDNA sequence of a precursor. *Proc. Natl. Acad. Sci. USA* **84**, 5449-5453.
Zasloff, M. (2009). Mysteries that still remain. *Biochim. Biophys. Acta* **1788**, 1693-1694.
Zhang, S., Wang, S., Li, H. and Li, L. (2011). Vitellogenin, a multivalent sensor and an antimicrobial effector. *Int. J. Biochem. Cell Biol.* **43**, 303-305.